

1 *Supplement for*

2 **Three-year characteristics of sulfuric acid in urban Beijing and**
3 **derivation of daytime sulfuric acid proxies applicable to various sites**

4

5 **Yishuo Guo et al.**

6 *Correspondence to: Chao Yan (chaoyan@nju.edu.cn), Yongchun Liu (liuyc@buct.edu.cn)*

7

8 Section S1. Measurement at Hyytiälä site

9 The boreal forest SMEAR II station is located at Hyytiälä, southern Finland (Hari and Kulmala, 2005; Hari et al.,
10 2013). The datasets used in this study are from 8th March to 13th August in 2018.

11 Sulfuric acid was measured by a CI-API-TOF mass spectrometry using nitric acid as reagent ions at the top of a
12 35 m tower. The calibration coefficient of sulfuric acid during the measurement period was $3.2 \times 10^9 \text{ molec cm}^{-3}$.
13 UVB radiation was also measured at the same height as sulfuric acid by a radiometer (Solar Light SL501A). The
14 particle number distributions of 3 - 1000 nm aerosols were obtained by a twin differential mobility particle sizer
15 (DMPS) (Aalto et al., 2001) at 8 m in height above ground, and was then used to calculate the condensation sink
16 (CS) according to the method from Kulmala et al. (Kulmala et al., 2001; Kulmala et al., 2012; Kerminen et al., 2001)
17 Besides, meteorological parameters and trace gases were continuously monitored at various heights (4.2, 8.4, 16.8,
18 33.6, 50.4, 67.2, 101, and 125 m) on a 126 m mast. Air temperature was measured by PT-100 resistance thermometer,
19 and air relative humidity (RH) was monitored by RH sensor (Rotronic HygroMet MP102H with HygroClip HC2S3,
20 Rotronic AG, Switzerland). SO₂ mixing ratio was monitored using an SO₂ fluorescence analyzer (Model 43i,
21 Thermo, USA). The temperature, RH and SO₂ measured at 33.6 m were utilized to match the height of sulfuric acid
22 and UVB.

23 Section S2. Estimation of hourly PM_{2.5} for Hyytiälä site

24 The mass concentrations of PM_{2.5} and PM₁₀ of Hyytiälä were continuously measured with the filter-sampled
25 Impactor, but they only had a resolution of 1–3 days. Meanwhile, the PM₁₀ was additionally monitored by a SHARP
26 instrument with hourly resolution. Therefore, it is possible to obtain the hourly PM_{2.5} data from hourly PM₁₀. We
27 then explore the relationship between PM_{2.5} and PM₁₀ from Impactor measurement. And as shown in Figure S12B,
28 PM_{2.5} had a very good linear correlation ($R = 1.0$) with PM₁₀ and the scaling factor between them was 0.8. Thus,
29 we calculated the hourly PM_{2.5} based on the equation of $\text{PM}_{2.5} = 0.8 \times \text{PM}_{10}$.

30 Section S3. Uncertainty analysis of sulfuric acid proxies

31 According to equation (4), the uncertainty of OH-CS based proxy can be calculated as follows:

$$32 \quad E_{\text{Proxy}_{\text{OH,CS}}} = \sqrt{(-0.7)^2 \cdot (E_T)^2 + (E_{\text{SO}_2})^2 + (E_{\text{OH}})^2 + (-1)^2 \cdot (E_{\text{CS}})^2}$$

33 The relationship between OH radical and UVB is $\text{OH} = 6.14 \times 10^6 \cdot \text{UVB}$. Then the uncertainty of replacing OH
34 radical by UVB is:

$$35 \quad E_{\text{UVB-substitution}} = \sqrt{(E_{\text{UVB-measure}})^2 + (E_{\text{UVB-to-OH}})^2 + (E_{\text{OH-modelling}})^2}$$

36 The relationship between CS and PM_{2.5} is $\text{CS} = 2.67 \times 10^{-3} \cdot \text{PM}_{2.5}^{2/3}$. Then the uncertainty of replacing CS by PM_{2.5}
37 is:

$$38 \quad E_{\text{PM}_{2.5}\text{-substitution}} = \sqrt{(2/3)^2 \cdot (E_{\text{PM}_{2.5}\text{-measure}})^2 + (E_{\text{PM}_{2.5}\text{-to-CS}})^2 + (E_{\text{CS}})^2}$$

The accuracies of measuring temperature (Vaisala) and PM_{2.5} (ThermoFisher) are usually smaller than 1% , and therefore can be ignored. The accuracies of measuring SO₂ (ThermoFisher) and UVB (KIPP&ZONEN) are around 1% and 5% respectively. The uncertainty of the model calculations of OH radical is approximately 40% (Tan et al., 2017;Ma et al., 2019;Ma et al., 2022). The underestimation of CS from DMPS measurement is around 11.7% (Figure S14, averaged relative errors of three periods). The relative error of using UVB to substitute OH radical is 86.5% (Figure S7A), and the relative error of using PM_{2.5} to substitute CS is 28.9% (Figure S7B). Bring those uncertainties of parameters into the above equations, we can get:

$$E_{\text{UVB-substitution}} = \sqrt{(E_{\text{UVB-measure}})^2 + (E_{\text{UVB-to-OH}})^2 + (E_{\text{OH-modelling}})^2} = \sqrt{(5\%)^2 + (86.5\%)^2 + (40\%)^2} = 95.4\%$$

$$E_{\text{PM}_{2.5}\text{-substitution}} = \sqrt{(E_{\text{PM}_{2.5}\text{-to-CS}})^2 + (E_{\text{CS}})^2} = \sqrt{(28.9\%)^2 + (11.7\%)^2} = 31.2\%$$

$$E_{\text{Proxy}_{\text{OH,CS}}} = \sqrt{(E_{\text{SO}_2})^2 + (E_{\text{OH}})^2 + (E_{\text{CS}})^2} = \sqrt{(1\%)^2 + (40\%)^2 + (11.7\%)^2} = 41.7\%$$

$$E_{\text{Proxy}_{\text{UVB,CS}}} = \sqrt{(E_{\text{SO}_2})^2 + (E_{\text{UVB-substitution}})^2 + (E_{\text{CS}})^2} = \sqrt{(1\%)^2 + (95.4\%)^2 + (11.7\%)^2} = 96.1\%$$

$$E_{\text{Proxy}_{\text{UVB,PM}_{2.5}}} = \sqrt{(E_{\text{SO}_2})^2 + (E_{\text{UVB-substitution}})^2 + (E_{\text{PM}_{2.5}\text{-substitution}})^2} = \sqrt{(1\%)^2 + (95.4\%)^2 + (31.2\%)^2} = 100.4\%$$

In summary, the uncertainties of OH-CS, UVB-CS and UVB-PM_{2.5} based proxies are estimated to be 41.7%, 96.1% and 100.4%, respectively.

54 Figures

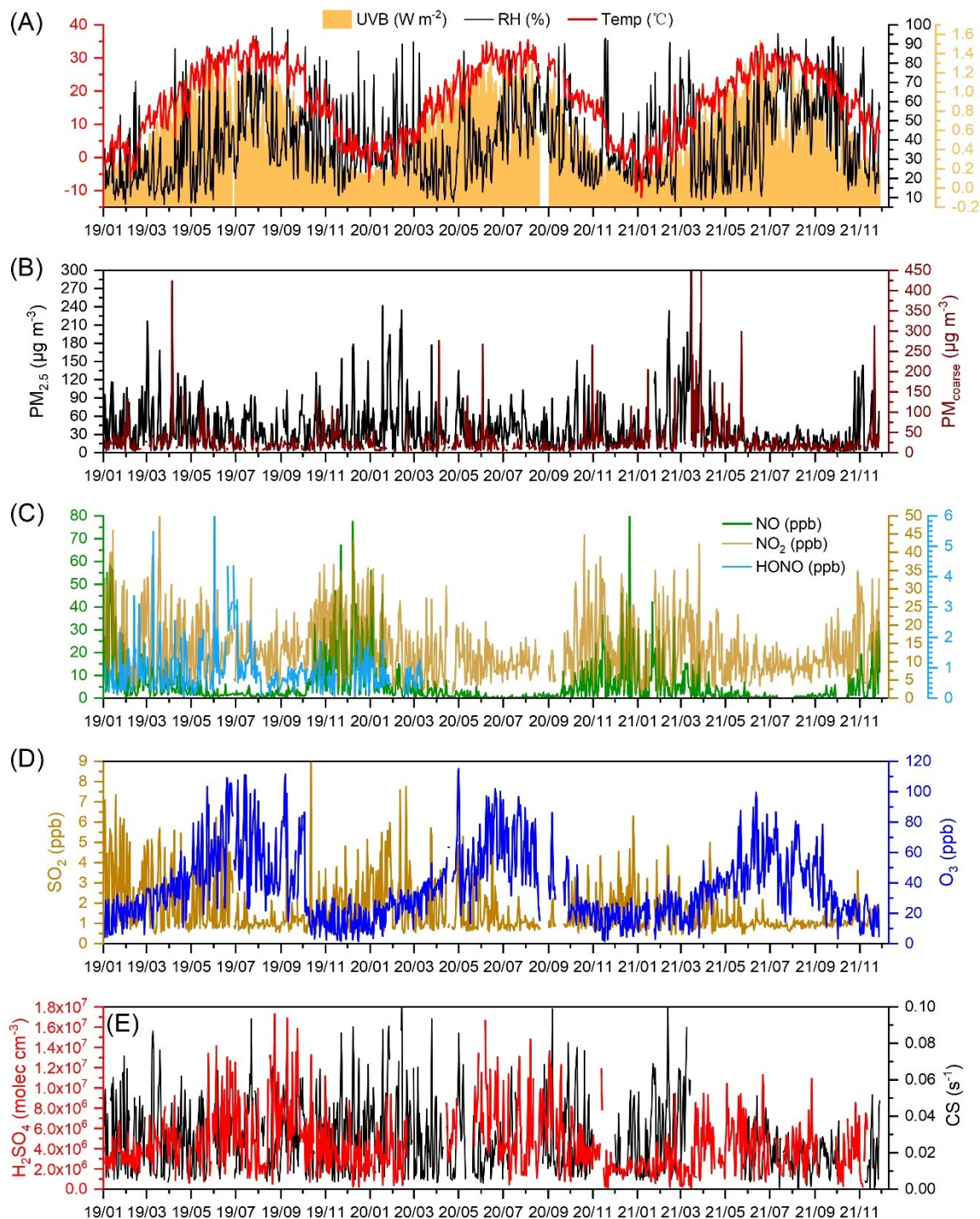


Figure S1. Three-year (from 2019 to 2021) time variations of (A) UVB, RH and temperature, (B) $\text{PM}_{2.5}$ and $\text{PM}_{\text{coarse}}$, (C) NO, NO_2 and HONO, (D) SO_2 and O_3 , and (E) sulfuric acid (H_2SO_4) and condensation sink (CS) during daytime (10:00-14:00). The labels on x-axes are in “year/month” format.

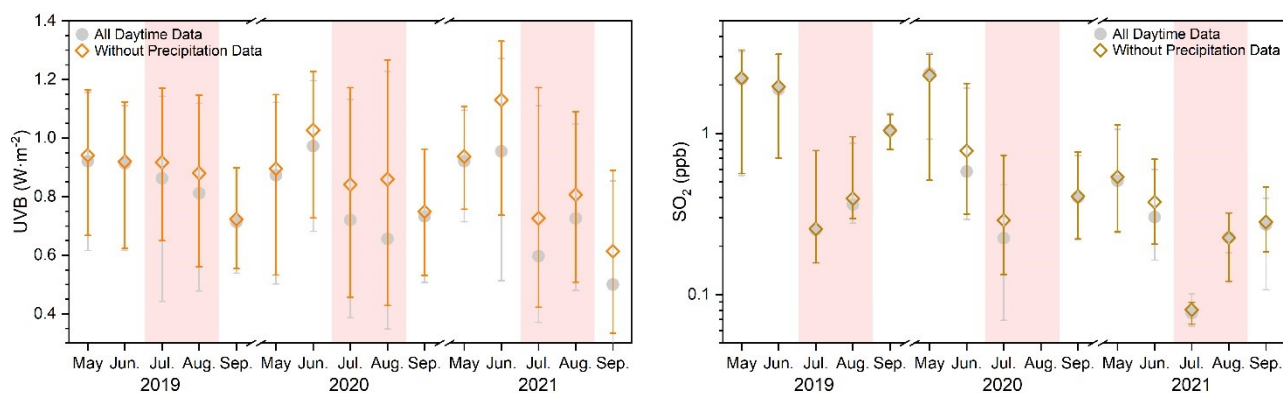


Figure S2. Monthly variations of UVB and SO₂ during daytime (10:00-14:00) in May, June, July, August and September in 2019, 2020 and 2021. The gray circles and orange diamonds represents datasets of all and without precipitation moments, respectively. The up line, middle marker and bottom line stand for upper quartile, median and lower quartile values respectively.

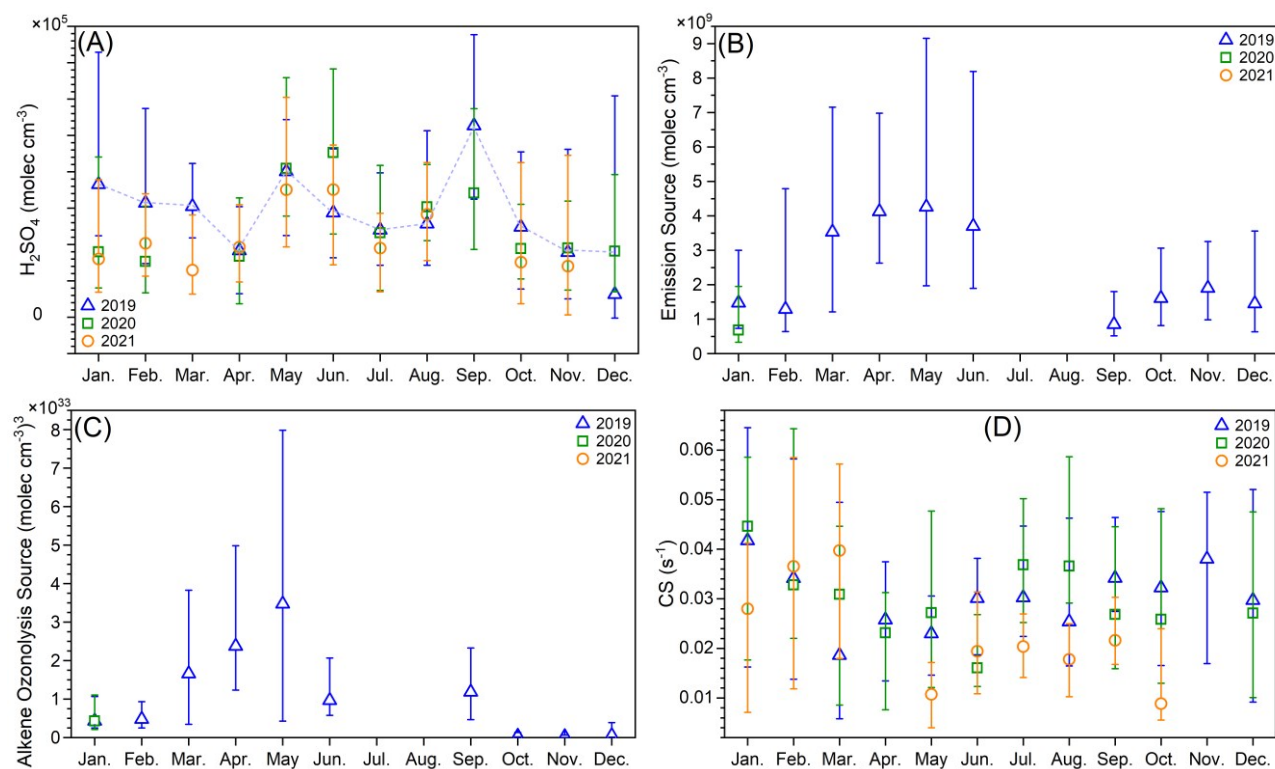


Figure S3. Three-year (from 2019 January to 2021 November) monthly variations of (A) H₂SO₄ concentration, (B) emission source of H₂SO₄ (Emission Source=[Benzene] $(\frac{WS}{1\text{ m s}^{-1}})^{1.398}(\frac{CS}{0.01\text{ s}^{-1}})^{-1.404}$ (Yang et al., 2021)), (C) alkene ozonolysis source of H₂SO₄ (Alkene Ozonolysis Source=[SO₂][O₃][Alkene] (Guo et al., 2021)) and (D) condensation sink (CS) during nighttime (22:00-02:00 next day). Blue triangles, green squares and orange circles represent data in 2019, 2020 and 2021, respectively. The up line, middle marker and bottom line stand for upper quartile, median and lower quartile values, respectively.

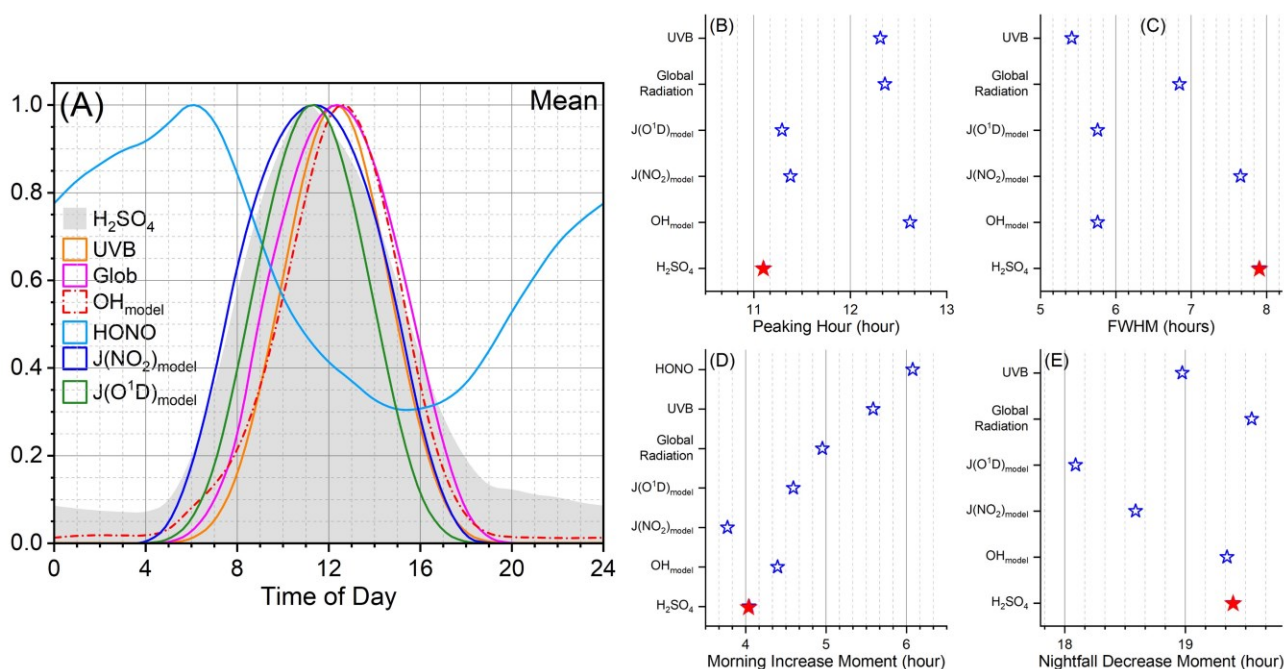


Figure S4. (A) Mean diurnal variations of H_2SO_4 , UVB, global radiation (Glob), modelled OH radical (OH_{model}), HONO, modelled photolysis rate of NO_2 ($J(NO_2)_{model}$) and modelled photolysis rate of O_3 to generate $O(^1D)$ ($J(O^1D)_{model}$) of 2019. The diurnal curves are depicted in normalized values. Values of (B) peaking hour, (C) full width at half maximum (FWHM), (D) morning increase moment, and (E) nightfall decrease moment from the curves of figure (A). Except from HONO, morning increase moment is when the diurnal curve starts increasing rapidly in the morning, and the nightfall decrease moment is when the diurnal curve turns from rapid to slow decreases at nightfall. For HONO, the “morning increase moment” is when HONO starts declining rapidly in the morning.

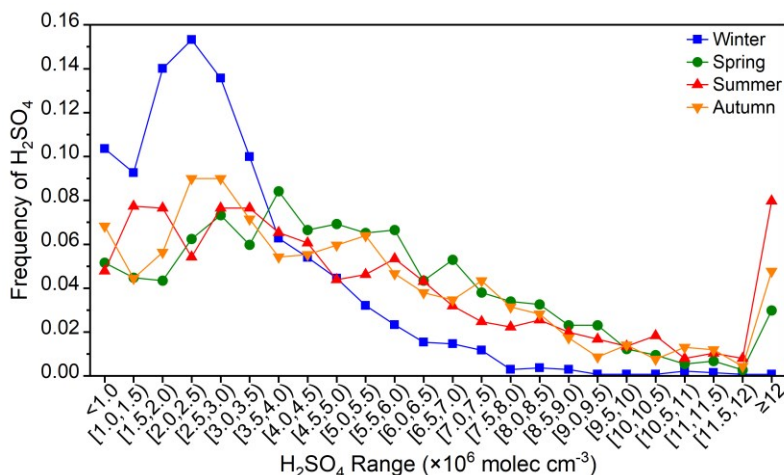


Figure S5. Distribution of daytime (10:00-14:00) sulfuric acid concentration in four seasons during three years (2019 to 2021).

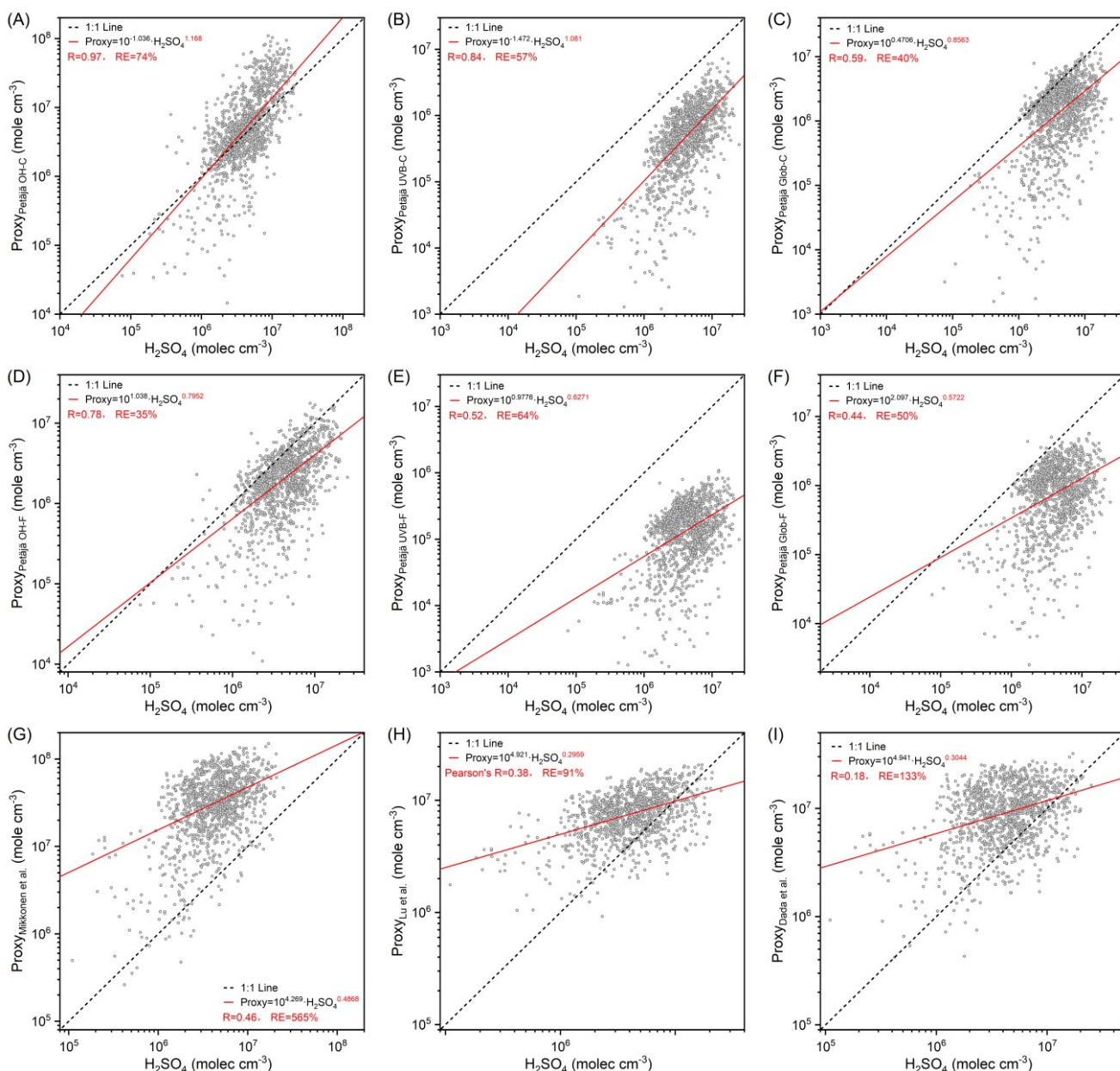


Figure S6. H_2SO_4 proxy suggested by (A) Petäjä et al., 2009 using OH radical with constant pre-factor k_1 , (B) Petäjä et al., 2009 using UVB with constant pre-factor k_2 , (C) Petäjä et al., 2009 using global radiation with constant pre-factor k_3 , (D) Petäjä et al., 2009 using OH radical with fitted pre-factor k_1 , (E) Petäjä et al., 2009 using UVB with fitted pre-factor k_2 , (F) Petäjä et al., 2009 using global radiation with fitted pre-factor k_3 , (G) Mikkonen et al., 2011 with equation N5, (H) Lu et al., 2019 with equation N7, and (I) Data et al., 2020 with the result of Figure 7(b) vs. measured H_2SO_4 during daytime (10:00-14:00) in 2019. In each plot, the black dashed lines are 1:1 lines, and the red lines are the least square fit lines between proxy and measured H_2SO_4 . Corresponding functions of the least square fit, correlation coefficients (R), and the relative error (RE) between proxies and measured H_2SO_4 are also shown in the legend.

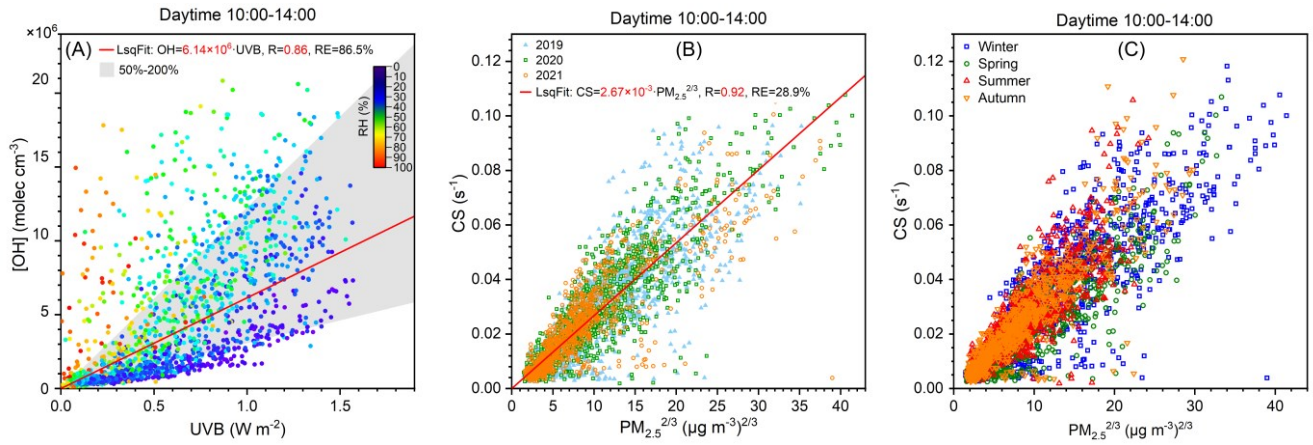
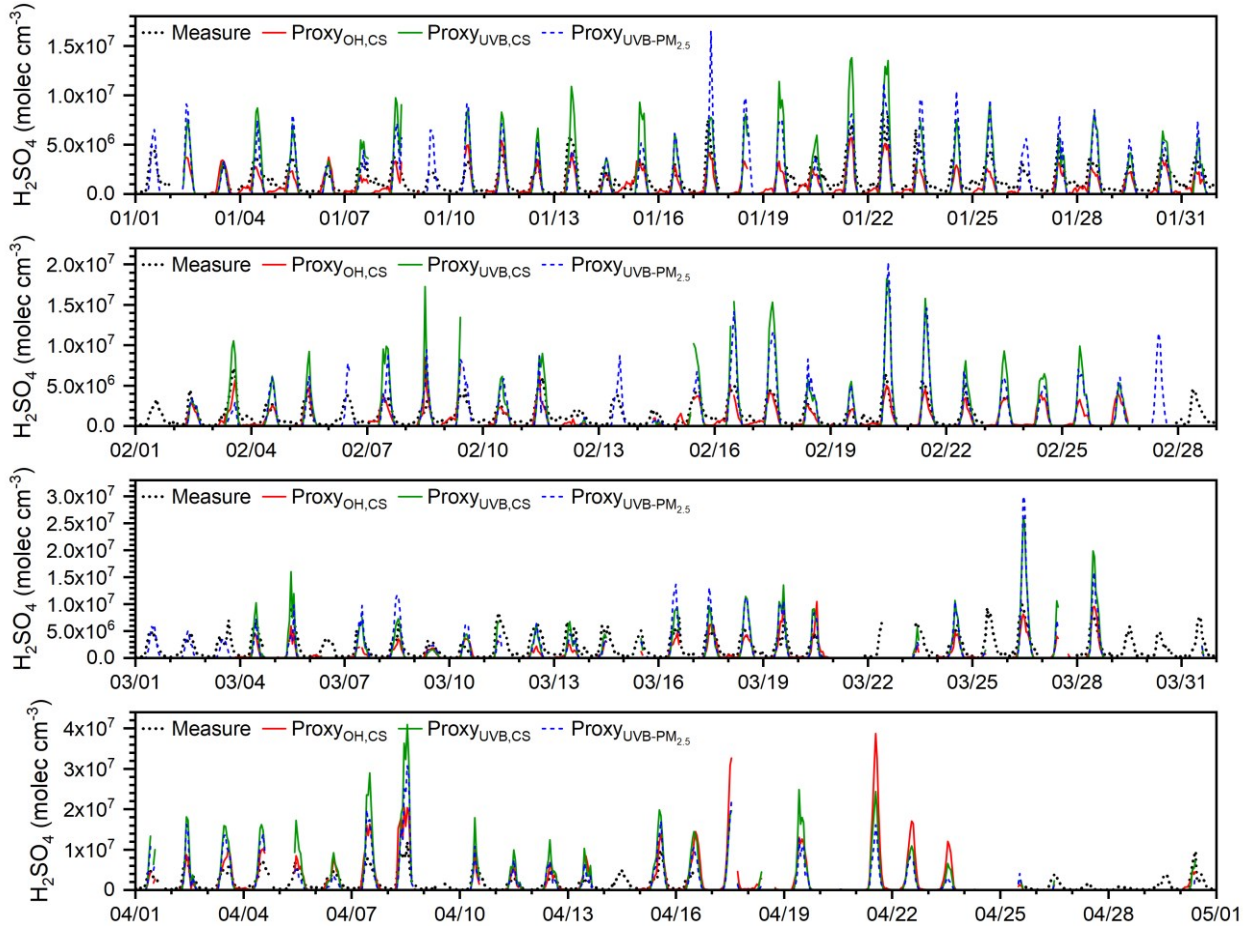
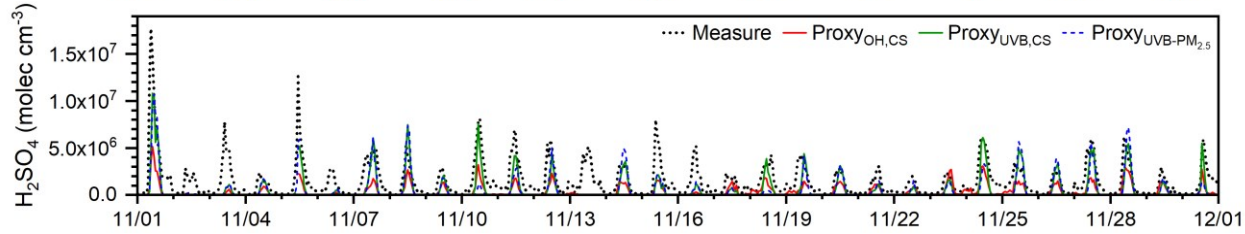
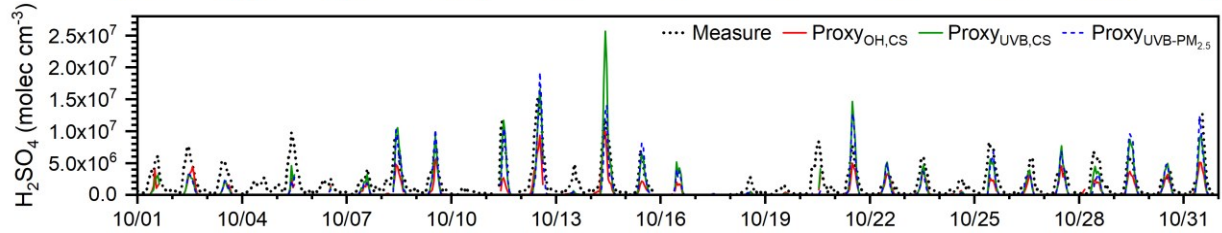
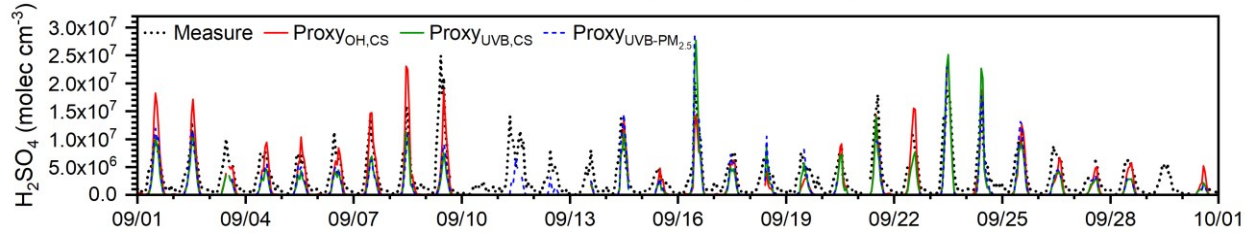
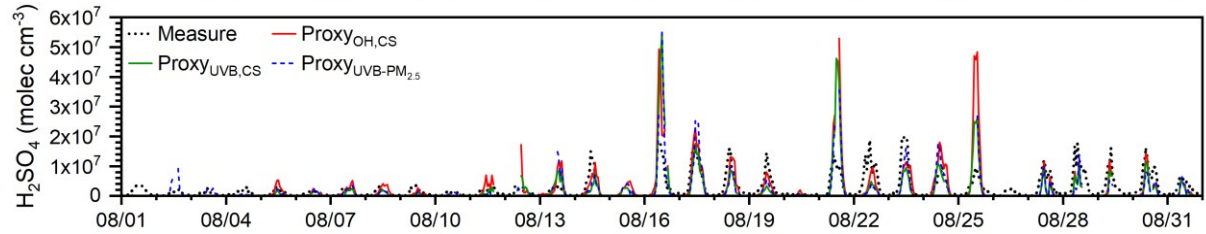
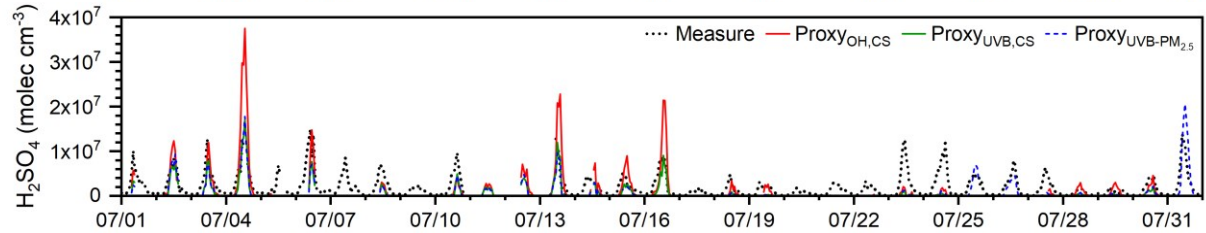
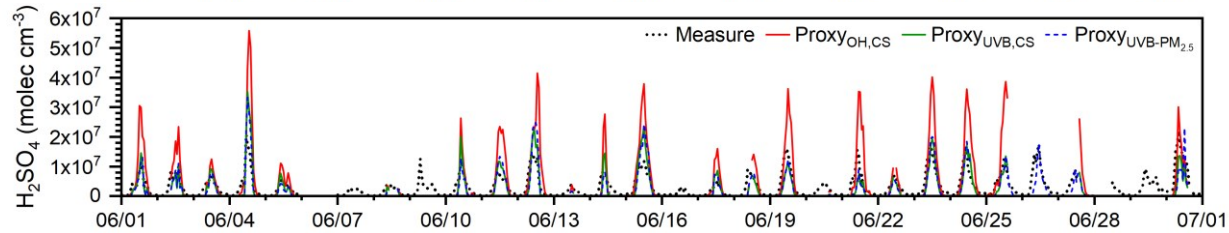
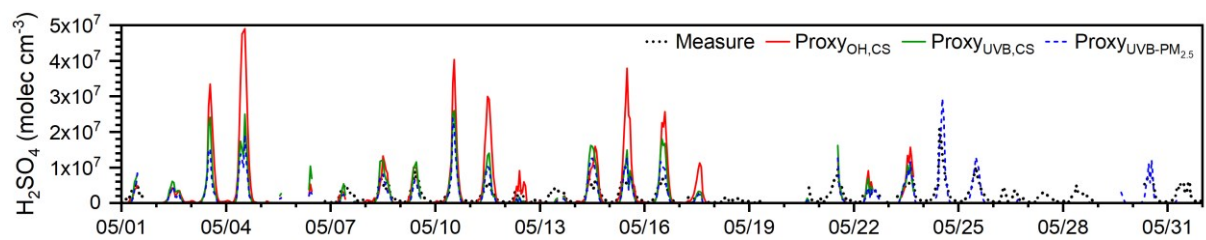


Figure S7. (A) Relationship between modelled OH radical and UVB colored by RH during daytime (10:00-14:00) in 2019. (B) and (C) Relationship between condensation sink (CS) and $\text{PM}_{2.5}^{2/3}$ during daytime from 2019 to 2021. In figure B, light blue triangle, hollow green square and hollow orange circle are for 2019, 2020 and 2021, respectively. In figure C, blue square, green circle, red upper triangle and orange lower triangle are for winter, spring, summer and autumn, respectively. Red lines are the least square fit lines between two parameters. The corresponding functions, correlation coefficients (R) and relative errors (RE) are shown in the legend. Gray area in figure A denotes 50% to 200% of the least square fitting.





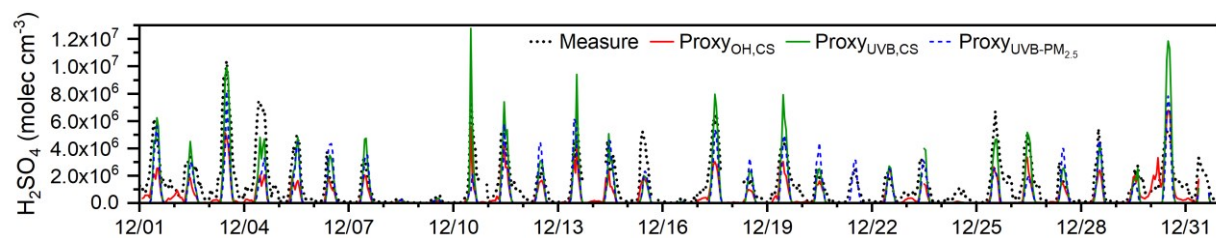
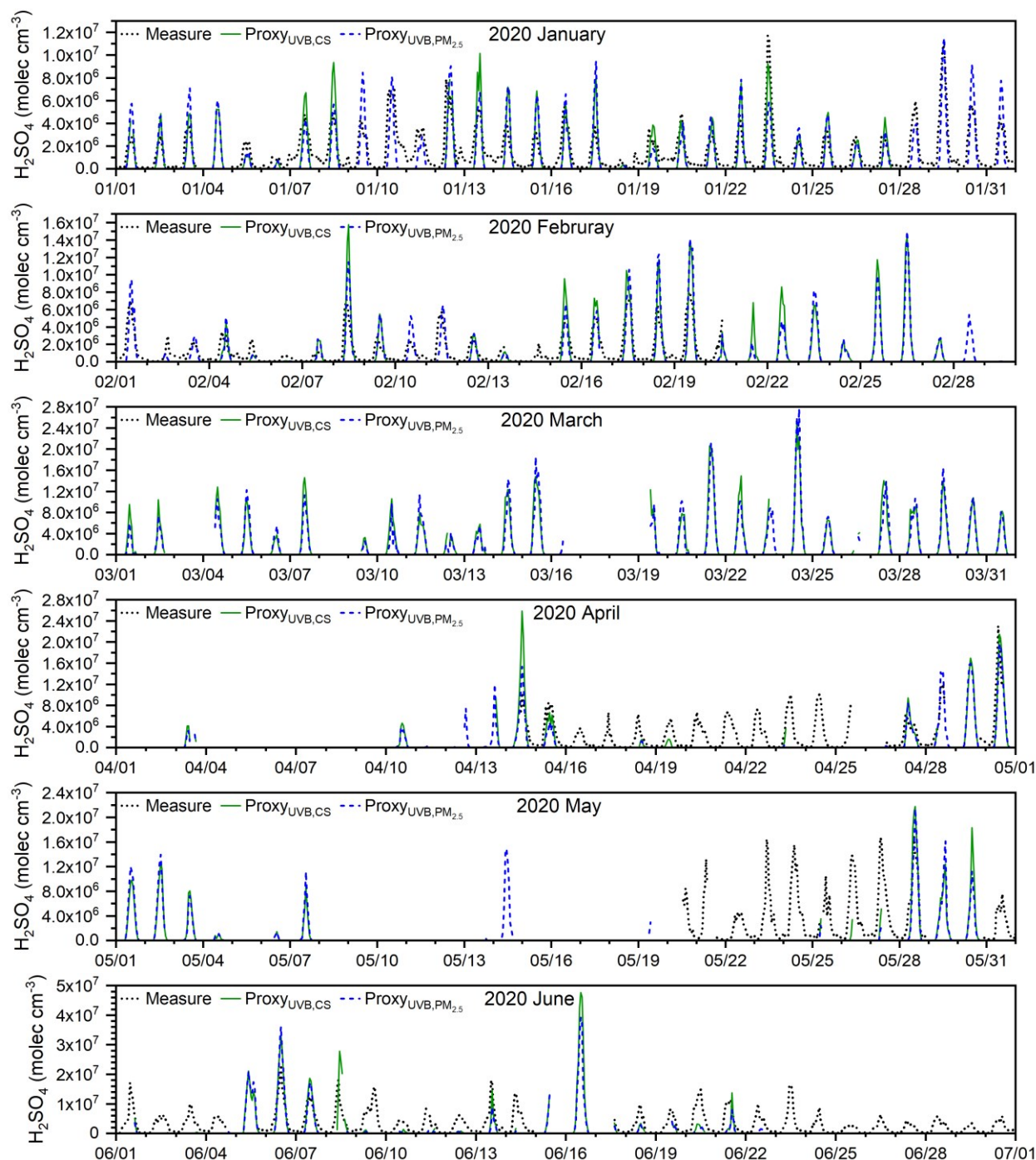
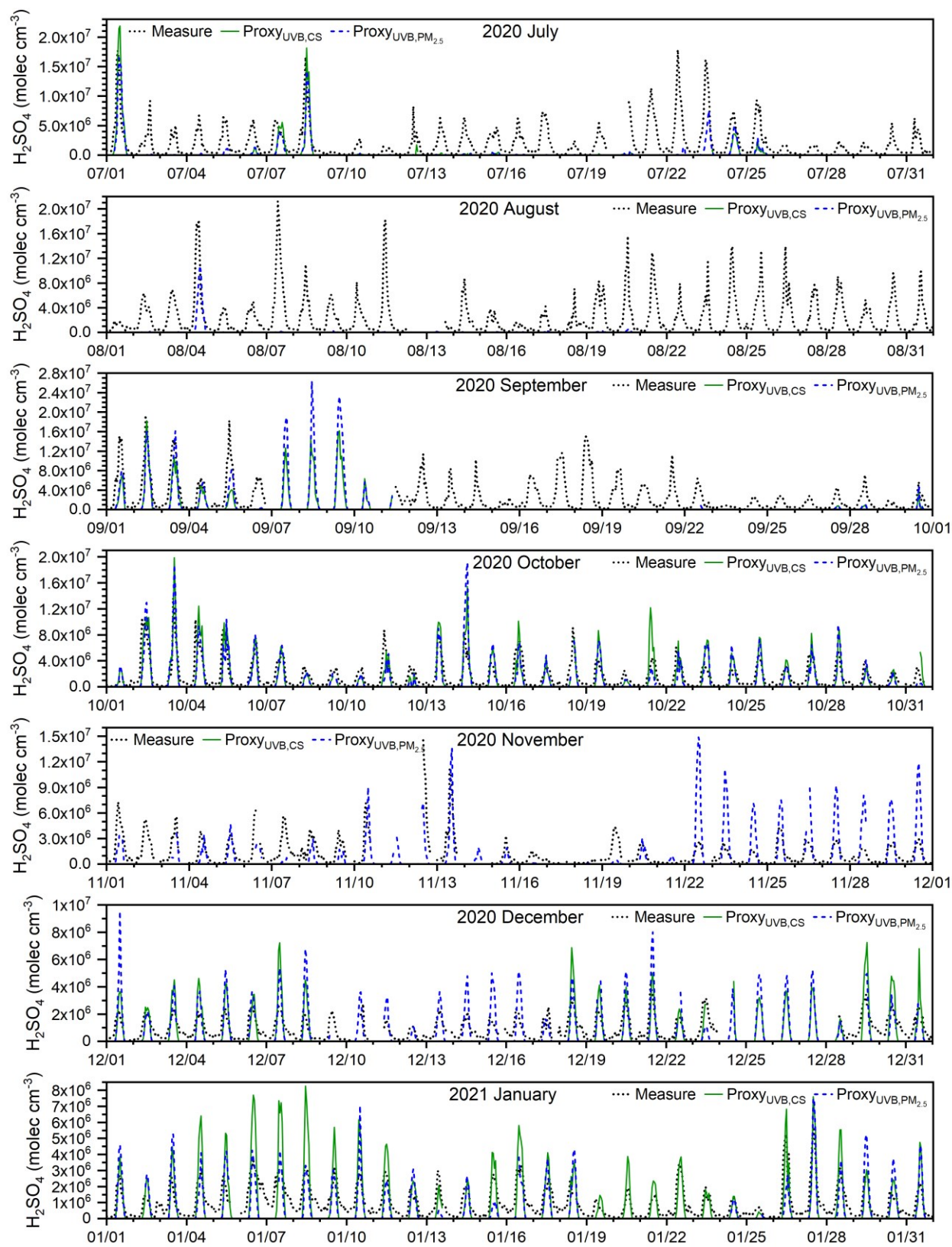
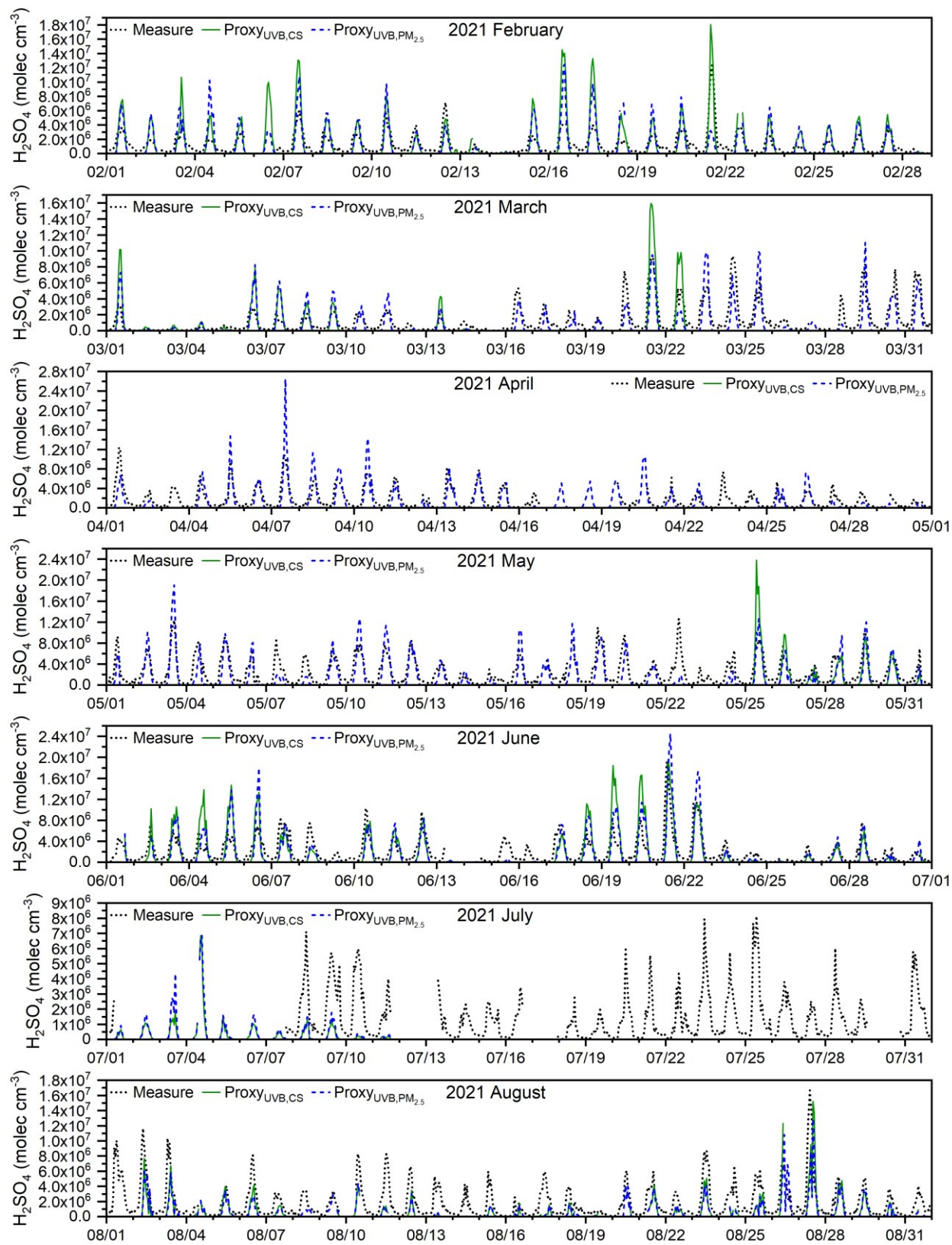


Figure S8. Time variation of measured sulfuric acid (Measure, black dashed line), OH-CS based proxy (Proxy_{OH,CS}, red line), UVB-CS based proxy (Proxy_{UVB,CS}, green line) and UVB-PM_{2.5} based proxy (Proxy_{UVB,PM_{2.5}}, blue dashed line) of sulfuric acid in 2019.







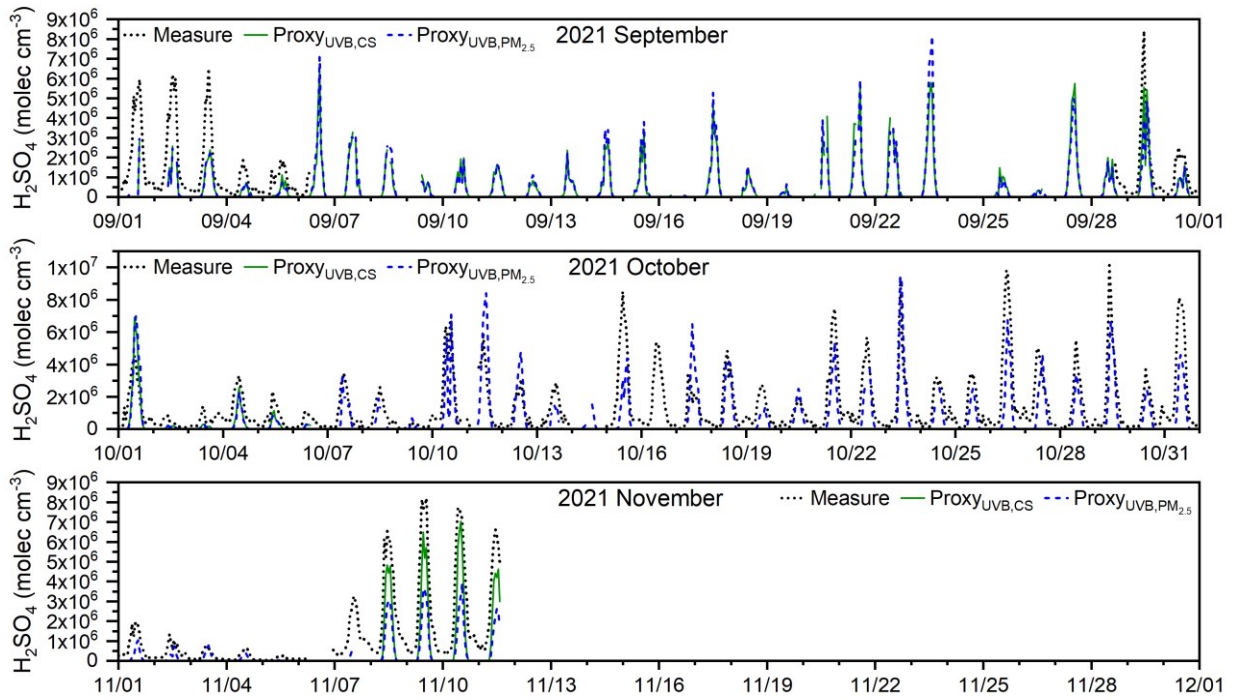
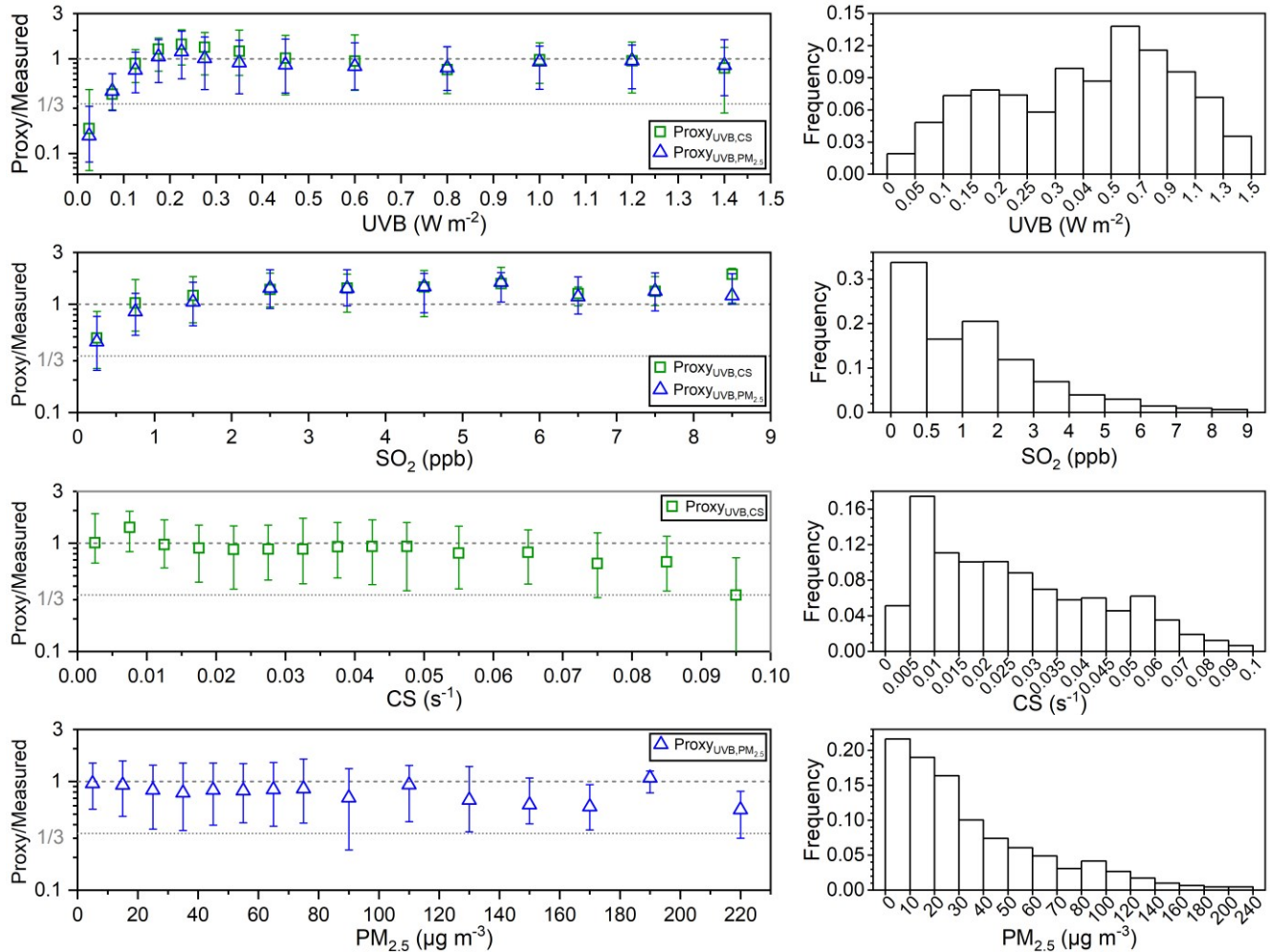


Figure S9. Time variations of measured sulfuric acid (Measure, black dashed line), UVB-CS based proxy ($\text{Proxy}_{\text{UVB,CS}}$, green line) and UVB- $\text{PM}_{2.5}$ based proxy ($\text{Proxy}_{\text{UVB,PM}_{2.5}}$, blue dashed line) of sulfuric acid in 2020 and 2021.



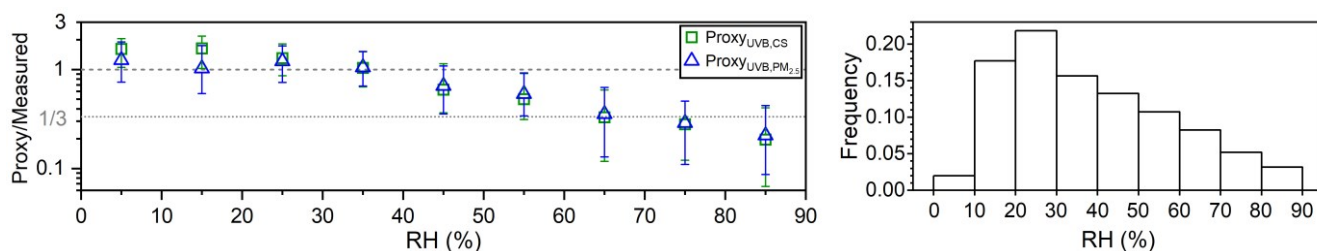


Figure S10. Left: The ratios of sulfuric acid concentrations estimated by proxies in this study to the measured one (Proxy/Measured) vs. UVB, SO_2 , CS, $\text{PM}_{2.5}$ and RH during daytime (10:00-14:00) of three years. Different colored markers represent different proxies. The up line, middle marker and bottom line stand for upper quartile, median and lower quartile values respectively. Right: Frequency distributions of corresponding parameters.

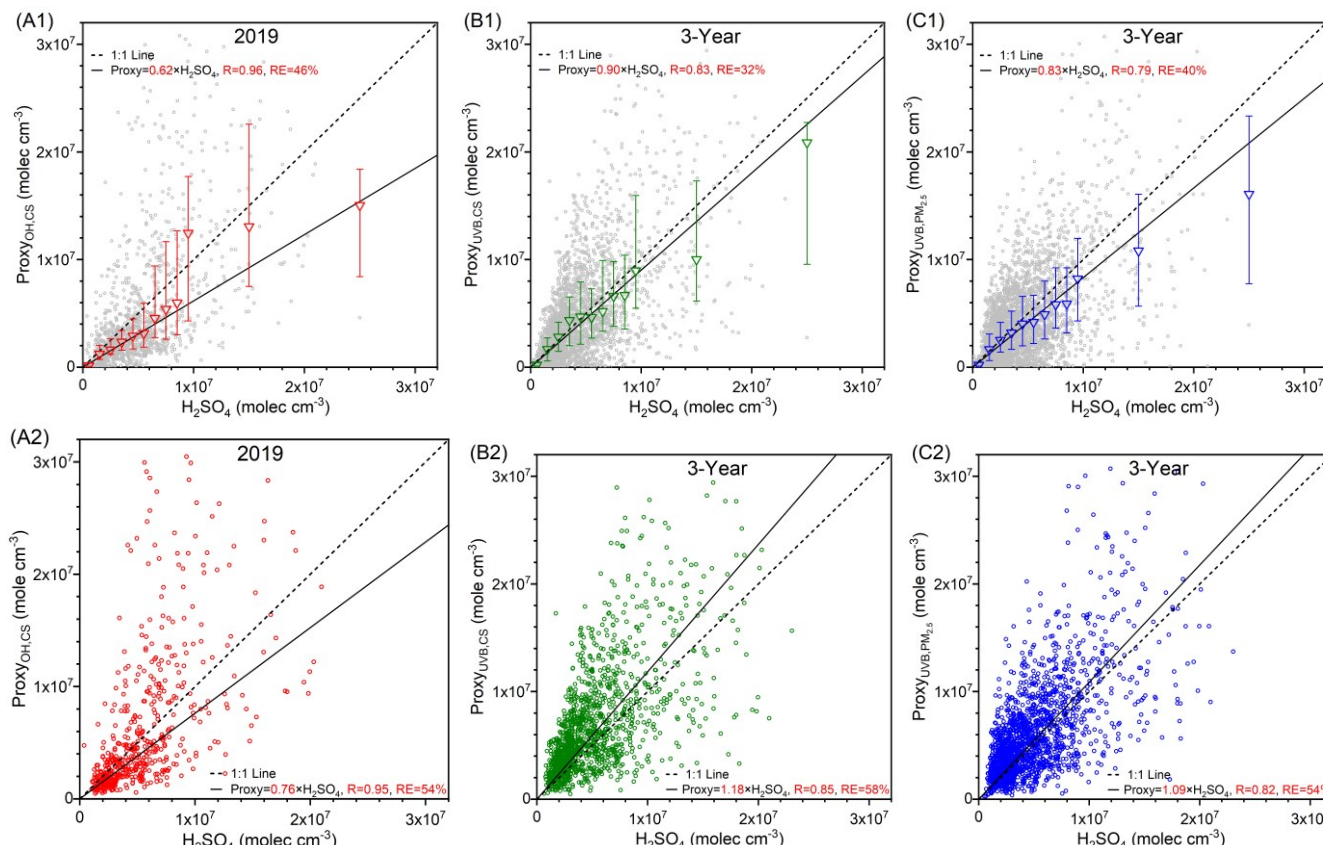


Figure S11. Sulfuric acid concentrations estimated by proxies vs. measured concentration during daytime (10:00-14:00) for (A1) and (A2) $\text{Proxy}_{\text{OH,CS}}$ in 2019, (B1) and (B2) $\text{Proxy}_{\text{UVB,CS}}$ in 3 years, and (C1) and (C2) $\text{Proxy}_{\text{UVB,PM}_{2.5}}$ in 3 years. The black dashed lines are 1:1 lines, and the black lines are the distance weighted least square fits between proxy and measured sulfuric acid. Corresponding functions of the fits, correlation coefficients (R) and relative errors (RE) are shown in the legend. For the first row, datasets include all daytime data. The triangle marker represents the binned data, where the up line, middle marker and bottom lines stand for upper quartile, median and lower quartile, respectively. For the second row, datasets only cover the optimal parameter ranges. Optimal parameter ranges for $\text{Proxy}_{\text{OH,CS}}$: $4 \times 10^5 < [\text{OH}] < 1.2 \times 10^7 \text{ mole cm}^{-3}$, $0.015 < \text{CS} < 0.07 \text{ s}^{-1}$, $\text{SO}_2 > 0.5 \text{ ppb}$ and $\text{RH} < 60\%$. Optimal parameter ranges for $\text{Proxy}_{\text{UVB,CS}}$: $\text{UVB} > 0.1 \text{ W m}^{-2}$, $\text{CS} < 0.07 \text{ s}^{-1}$, $\text{SO}_2 > 0.5 \text{ ppb}$ and $\text{RH} < 60\%$. Optimal parameter ranges for $\text{Proxy}_{\text{UVB,PM}_{2.5}}$: $\text{UVB} > 0.1 \text{ W m}^{-2}$, $\text{PM}_{2.5} < 200 \mu\text{g m}^{-3}$, $\text{SO}_2 > 0.5 \text{ ppb}$ and $\text{RH} < 60\%$.

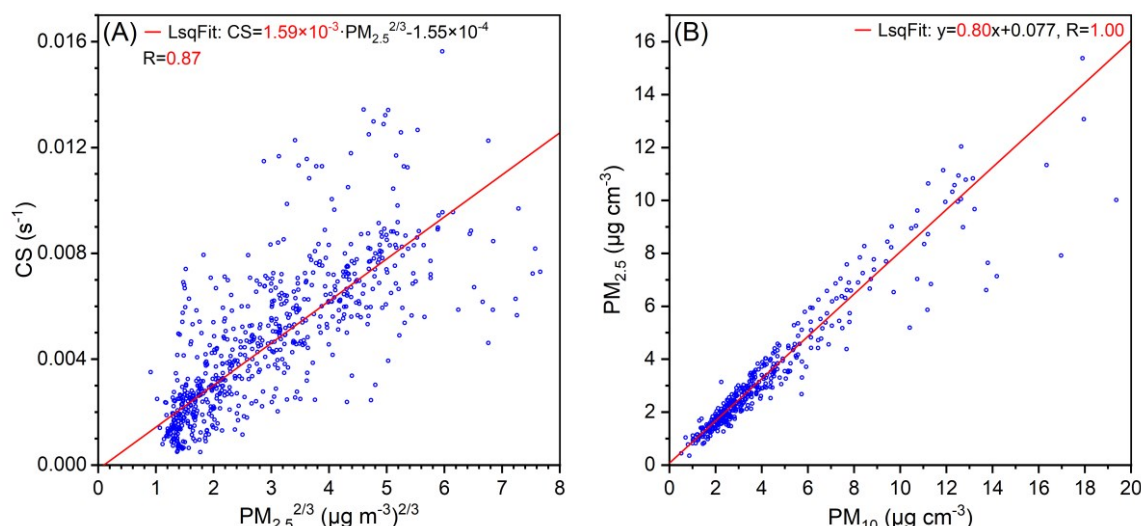


Figure S12. (A) Relationship between condensation sink (CS) and $PM_{2.5}^{2/3}$ for Hyytiälä site during daytime (10:00–14:00) from 8th March to 13th Aug. 2018. (B) Relationship between daily $PM_{2.5}$ and daily PM_{10} for Hyytiälä site from 2017 to 2019. In both two plots, the red lines are the least square fit lines between two parameters. Corresponding functions of the fits and correlation coefficients (R) are also shown in the legend.

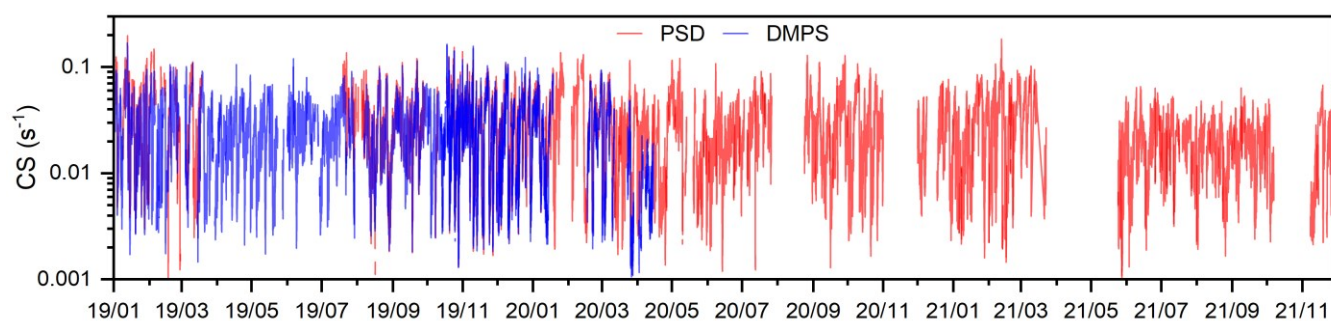


Figure S13. Three-year (from 2019 to 2021) time variations of condensation sink (CS) calculated from the particle number size distribution of PSD and DMPS. The labels on x-axes are in “year/month” format.

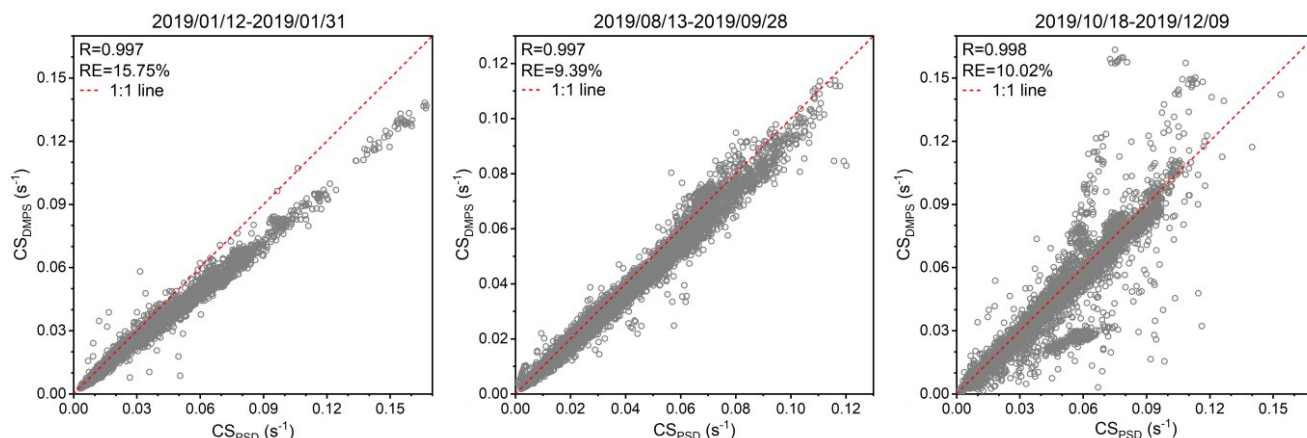


Figure S14. Correlation between condensation sinks (CS) calculated from DMPS with size ranges of 6–840 nm and PSD with size ranges of 3 nm–10 μ m during three periods with continuous and stable measurement. The correlation coefficients (R) and relative errors between them are listed in the legend.

190 Tables

191 **Table S1.** Precipitation frequency during daytime (10:00-14:00) in May, June, July, August and September in 2019, 2020 and
192 2021.

Month	2019	2020	2021
May	4%	14%	8%
June	5%	15%	25%
July	19%	21%	37%
August	13%	20%	26%
September	5%	12%	24%

193 **Table S2.** Monthly concentration of H_2SO_4 (molec cm^{-3}) during nighttime (22:00-02:00 next day) from 2019 to 2021. “NaN”
194 means there is no data available.
195

Month	2019			2020			2021		
	Median	25th	75th	Median	25th	75th	Median	25th	75th
January	4.7×10^5	3.2×10^5	8.3×10^5	2.8×10^5	1.8×10^5	5.4×10^5	2.6×10^5	1.7×10^5	4.8×10^5
February	4.1×10^5	2.5×10^5	6.7×10^5	2.5×10^5	1.7×10^5	4.1×10^5	3.0×10^5	2.1×10^5	4.4×10^5
March	4.0×10^5	3.2×10^5	5.2×10^5	NaN	NaN	NaN	2.3×10^5	1.6×10^5	3.8×10^5
April	2.8×10^5	1.6×10^5	4.0×10^5	2.7×10^5	1.4×10^5	4.3×10^5	2.9×10^5	2.0×10^5	4.1×10^5
May	5.0×10^5	3.3×10^5	6.4×10^5	5.1×10^5	3.8×10^5	7.6×10^5	4.5×10^5	2.9×10^5	7.0×10^5
June	3.9×10^5	2.6×10^5	5.6×10^5	5.5×10^5	3.3×10^5	7.8×10^5	4.5×10^5	2.4×10^5	5.7×10^5
July	3.4×10^5	2.4×10^5	5.0×10^5	3.3×10^5	1.7×10^5	5.2×10^5	2.9×10^5	1.7×10^5	3.9×10^5
August	3.6×10^5	2.4×10^5	6.1×10^5	4.0×10^5	3.1×10^5	5.2×10^5	3.8×10^5	2.6×10^5	5.3×10^5
September	6.3×10^5	4.2×10^5	8.8×10^5	4.4×10^5	2.9×10^5	6.7×10^5	NaN	NaN	NaN
October	3.5×10^5	1.8×10^5	5.6×10^5	2.9×10^5	2.1×10^5	4.1×10^5	2.5×10^5	1.4×10^5	5.3×10^5
November	2.8×10^5	1.5×10^5	5.6×10^5	2.9×10^5	1.7×10^5	4.2×10^5	2.4×10^5	1.1×10^5	5.5×10^5
December	1.6×10^5	9.8×10^4	7.1×10^5	2.8×10^5	1.7×10^5	4.9×10^5	NaN	NaN	NaN

196 **Table S3.** Mean, standard deviation (Std), median, lower quartile (25th) and upper quartile (75th) of sulfuric acid concentrations
197 from measurement and estimated by proxies from literatures during the time window of 10:00-14:00 in 2019 (1st January to
198 31st December). The unit of concentration is molec cm^{-3} .
199

Parameters		Mean	Std	Median	25th	75th
Measured H_2SO_4		4.9×10^6	3.5×10^6	3.9×10^6	2.5×10^6	6.3×10^6
H_2SO_4 Proxy	Proxy Petäjä OH-C	1.0×10^7	1.4×10^7	4.7×10^6	2.5×10^6	1.1×10^7
	Proxy Petäjä OH-F	2.8×10^6	2.6×10^6	2.1×10^6	1.2×10^6	3.5×10^6
	Proxy Petäjä UVB-C	7.7×10^5	8.0×10^5	5.5×10^5	2.7×10^5	1.0×10^6
	Proxy Petäjä UVB-F	1.9×10^5	1.5×10^5	1.6×10^5	7.2×10^4	2.7×10^5
	Proxy Petäjä Glob-C	2.1×10^6	1.8×10^6	1.7×10^6	7.4×10^5	3.0×10^6
	Proxy Petäjä Glob-F	1.1×10^6	9.0×10^5	9.0×10^5	3.9×10^5	1.6×10^6
	Proxy Mikkonen et al.	3.9×10^7	2.6×10^7	3.4×10^7	1.9×10^7	5.2×10^7
	Proxy Lu et al.	8.3×10^6	3.7×10^6	7.8×10^6	5.6×10^6	1.0×10^7
	Proxy Dada et al.	1.1×10^7	5.8×10^6	9.7×10^6	6.0×10^6	1.4×10^7

200 **Table S4.** Mean, standard deviation (Std), median, lower quartile (25th) and upper quartile (75th) of sulfuric acid concentrations
201 from measurement and estimated by proxies in this study during daytime (10:00-14:00). The concentrations in 2019, 2020,
202 2021 and 3 years are summarized respectively. The unit of concentration is molec cm^{-3} .
203

Year	Parameters	Mean	Std	Median	25th	75th
2019	$[\text{H}_2\text{SO}_4]_{2019}$	4.9×10^6	3.5×10^6	3.9×10^6	2.5×10^6	6.3×10^6
	$\text{Proxy}_{\text{OH,CS}}$	6.0×10^6	8.2×10^6	2.8×10^6	1.5×10^6	6.3×10^6
3-Year	$[\text{H}_2\text{SO}_4]_{3\text{-Year}}$	4.4×10^6	3.3×10^6	3.5×10^6	2.1×10^6	5.8×10^6
	$\text{Proxy}_{\text{UVB,CS}}$	5.1×10^6	5.5×10^6	3.6×10^6	1.5×10^6	6.9×10^6
	$\text{Proxy}_{\text{UVB,PM}_{2.5}}$	4.5×10^6	4.7×10^6	3.2×10^6	1.3×10^6	6.1×10^6

205 References

- 206 Aalto, P., Hämeri, K., Becker, E., Weber, R., Salm, J., Mäkelä, J. M., Hoell, C., O’ Dowd, C. D., Hansson, H.-C., Väkevä, M.,
 207 Koponen, I. K., Buzorius, G., and Kulmala, M.: Physical characterization of aerosol particles during nucleation events, *Tellus*
 208 B: Chemical and Physical Meteorology, 53, 344-358, 10.3402/tellusb.v53i4.17127, 2001.
- 209 Guo, Y., Yan, C., Li, C., Ma, W., Feng, Z., Zhou, Y., Lin, Z., Dada, L., Stolzenburg, D., Yin, R., Kontkanen, J., Daellenbach,
 210 K. R., Kangasluoma, J., Yao, L., Chu, B., Wang, Y., Cai, R., Bianchi, F., Liu, Y., and Kulmala, M.: Formation of nighttime
 211 sulfuric acid from the ozonolysis of alkenes in Beijing, *Atmospheric Chemistry and Physics*, 21, 5499-5511, 10.5194/acp-21-
 212 5499-2021, 2021.
- 213 Hari, P., and Kulmala, M.: Station for Measuring Ecosystem-Atmosphere Relations (SMEAR II), *Boreal Environment*
 214 Research, 10, 315-322, 2005.
- 215 Hari, P., Nikinmaa, E., Pohja, T., Siivola, E., Bäck, J., Vesala, T., and Kulmala, M.: Station for Measuring Ecosystem-
 216 Atmosphere Relations: SMEAR, in: *Physical and Physiological Forest Ecology*, edited by: Hari, P., Heliövaara, K., and
 217 Kulmala, L., Springer Netherlands, Dordrecht, 471-487, 2013.
- 218 Kerminen, V.-M., Pirjola, L., and Kulmala, M.: How significantly does coagulative scavenging limit atmospheric particle
 219 production?, *Journal of Geophysical Research: Atmospheres*, 106, 24119-24125, <https://doi.org/10.1029/2001JD000322>, 2001.
- 220 CUV5 and SUV Series Ultraviolet Radiometers: <https://www.kippzonen.com/Product/363/SUV5-Total-UV-Radiometer>.
- 221 Kulmala, M., Maso, M. D., Mäkelä, J. M., Pirjola, L., Väkevä, M., Aalto, P., Miikkulainen, P., Hämeri, K., and O’ Dowd, C.
 222 D.: On the formation, growth and composition of nucleation mode particles, *Tellus B: Chemical and Physical Meteorology*, 53,
 223 479-490, 10.3402/tellusb.v53i4.16622, 2001.
- 224 Kulmala, M., Petäjä, T., Nieminen, T., Sipilä, M., Manninen, H. E., Lehtipalo, K., Dal Maso, M., Aalto, P. P., Junninen, H.,
 225 Paasonen, P., Riipinen, I., Lehtinen, K. E. J., Laaksonen, A., and Kerminen, V.-M.: Measurement of the nucleation of
 226 atmospheric aerosol particles, *Nature Protocols*, 7, 1651-1667, 10.1038/nprot.2012.091, 2012.
- 227 Ma, X., Tan, Z., Lu, K., Yang, X., Liu, Y., Li, S., Li, X., Chen, S., Novelli, A., Cho, C., Zeng, L., Wahner, A., and Zhang, Y.:
 228 Winter photochemistry in Beijing: Observation and model simulation of OH and HO₂ radicals at an urban site, *Science of The*
 229 *Total Environment*, 685, 85-95, <https://doi.org/10.1016/j.scitotenv.2019.05.329>, 2019.
- 230 Ma, X., Tan, Z., Lu, K., Yang, X., Chen, X., Wang, H., Chen, S., Fang, X., Li, S., Li, X., Liu, J., Liu, Y., Lou, S., Qiu, W.,
 231 Wang, H., Zeng, L., and Zhang, Y.: OH and HO₂ radical chemistry at a suburban site during the EXPLORE-YRD campaign
 232 in 2018, *Atmospheric Chemistry and Physics*, 22, 7005-7028, 10.5194/acp-22-7005-2022, 2022.
- 233 Tan, Z., Fuchs, H., Lu, K., Hofzumahaus, A., Bohn, B., Broch, S., Dong, H., Gomm, S., Häseler, R., He, L., Holland, F., Li,
 234 X., Liu, Y., Lu, S., Rohrer, F., Shao, M., Wang, B., Wang, M., Wu, Y., Zeng, L., Zhang, Y., Wahner, A., and Zhang, Y.:
 235 Radical chemistry at a rural site (Wangdu) in the North China Plain: Observation and model calculations of OH, HO₂ and RO₂
 236 radicals, *Atmospheric Chemistry and Physics*, 17, 663-690, 10.5194/acp-17-663-2017, 2017.
- 237 TEOM 1405-D Ambient Particulate Monitor: [https://www.thermofisher.cn/order/catalog/product/TEOM1405DF?SID=srch-](https://www.thermofisher.cn/order/catalog/product/TEOM1405DF?SID=srch-srp-TEOM1405DF)
 238 [srp-TEOM1405DF](https://www.thermofisher.cn/order/catalog/product/TEOM1405DF).
- 239 Thermo Scientific Model 43i-TLE: <https://www.thermofisher.cn/order/catalog/product/43ITLE?SID=srch-hj-43i-TLE>.
- 240 Relative Humidity and Temperature Probe HMP4: [https://www.vaisala.com/en/products/instruments-sensors-and-other-](https://www.vaisala.com/en/products/instruments-sensors-and-other-measurement-devices/instruments-industrial-measurements/hmp4)
 241 [measurement-devices/instruments-industrial-measurements/hmp4](https://www.vaisala.com/en/products/instruments-sensors-and-other-measurement-devices/instruments-industrial-measurements/hmp4).
- 242 Yang, L., Nie, W., Liu, Y., Xu, Z., Xiao, M., Qi, X., Li, Y., Wang, R., Zou, J., Paasonen, P., Yan, C., Xu, Z., Wang, J., Zhou,
 243 C., Yuan, J., Sun, J., Chi, X., Kerminen, V.-M., Kulmala, M., and Ding, A.: Toward building a physical proxy for gas-phase
 244 sulfuric acid concentration based on its budget analysis in polluted Yangtze River Delta, East China, *Environmental Science*
 245 *& Technology*, 55, 6665-6676, 10.1021/acs.est.1c00738, 2021.